


 Cite this: *Nanoscale*, 2024, **16**, 19266

## An ionic Cu<sub>9</sub>Na<sub>4</sub>-phenylsilsesquioxane/ bis(triphenylphosphine)iminium complex: synthesis, unique structure, and catalytic activity†

 Alexey N. Bilyachenko, <sup>\*a,b</sup> Victor N. Khrustalev, <sup>b,c</sup> Zhibin Huang, <sup>b</sup>  
 Kristina D. Dubinina, <sup>b</sup> Elena S. Shubina, <sup>a</sup> Nikolai N. Lobanov, <sup>b</sup> Di Sun, <sup>d</sup>  
 Elisabete C. B. A. Alegria <sup>e,f</sup> and Armando J. L. Pombeiro\*<sup>f</sup>

The synthesis of a high nuclear (Cu<sub>9</sub>Na<sub>4</sub>) complex **1** via the self-assembly of copper(II) phenylsilsesquioxane induced by complexation with bis(triphenylphosphine)iminium chloride (PPNCl) was successfully achieved. This complex, which includes two bis(triphenylphosphine)iminium PPN<sup>+</sup> cations, represents the first example of a metallasilsesquioxane/phosphazene compound. The Cu<sub>9</sub>Na<sub>4</sub>-silsesquioxane cage demonstrates a nontrivial combination of two pairs of Si<sub>6</sub>-cyclic/Si<sub>4</sub>-acyclic silsesquioxane ligands and a fusion of two Si<sub>10</sub>Cu<sub>4</sub>Na<sub>2</sub> fragments, combined via the central ninth copper ion. The catalytic efficacy of the copper(II) compound (**1**) was evaluated through the peroxidative oxidation of toluene using *tert*-butyl hydroperoxide (*t*-BuOOH) as the oxidant. The primary oxidation products were benzaldehyde (BAL), benzyl alcohol (BOL), and benzoic acid (BAC), with BAC being the predominant product, especially in acetonitrile (NCMe). The formation of cresols, indicating oxidation at the aromatic ring, was observed only in water and under microwave irradiation (MW) in NCMe. Remarkably, the highest total yield of 40.3% was achieved in water with an acidic additive at 80 °C, highlighting the crucial role of the acid additive in enhancing reaction efficiency and selectivity. This study underscores our copper(II) complex as a highly effective catalyst for toluene oxidation, demonstrating its significant potential for fine-tuning reaction parameters to optimize yields and selectivity. The unprecedented structure of the complex and its promising catalytic performance pave the way for further advancements in the fields of metallasilsesquioxane chemistry and catalysis.

 Received 1st June 2024,  
 Accepted 3rd September 2024

DOI: 10.1039/d4nr02298j

[rsc.li/nanoscale](https://rsc.li/nanoscale)

## Introduction

Cage-like metallasilsesquioxanes (CLMSs) are a fast-growing family of metallacomplexes with impressive molecular aes-

thetics.<sup>1</sup> Multiplicity of nuclearities, compositions, and structures various multiple functionalities to CLMSs. Important physical properties of CLMSs include magnetic (single-molecule magnet and spin glass behaviors)<sup>2</sup> and luminescence properties (with examples of ratiometric luminescent thermometers).<sup>3</sup> CLMSs are suitable for the design of functional coordination polymers<sup>4</sup> and other important materials (semiconductors,<sup>5</sup> photoswitches,<sup>6</sup> fungicides,<sup>7</sup> ceramic silicates,<sup>8</sup> and objects with flame-retardance/intumescence properties<sup>9</sup>). In addition to sporadic reports on CLMS-involved activation of small molecules,<sup>2e,10</sup> numerous works are devoted to the catalytic properties of CLMSs.<sup>11</sup> These include recent reports on their activity in the Baeyer–Villiger reaction,<sup>12</sup> tandem deacetalization/deketalization-Knoevenagel condensation reactions,<sup>13</sup> synthesis of quinazolinones,<sup>14</sup> or amidations.<sup>15</sup>

Keeping in mind the reported activity of copper complex catalysts<sup>16</sup> and rich opportunities for the design of copper silsesquioxane architectures via complexation with auxiliary organic ligands,<sup>17</sup> we decided to develop new types of mixed ligand copper silsesquioxane complexes with potential catalytic activity in transformations of volatile organic compounds (VOCs).

<sup>a</sup>A.N. Nesmeyanov Institute of Organoelement Compounds, Russian Academy of Sciences, Vavilov Street 28, 119991 Moscow, Russia.

E-mail: bilyachenko@ineos.ac.ru

<sup>b</sup>Peoples' Friendship University of Russia (RUDN University), Miklukho-Maklay Str. 6, 117198 Moscow, Russia

<sup>c</sup>Zelinsky Institute of Organic Chemistry, Russian Academy of Sciences, Leninsky Prospect 47, 119991 Moscow, Russia

<sup>d</sup>Shandong University, Department of Chemistry and Chemical Engineering, Shanda South Road 27, 250100 Jinan, China

<sup>e</sup>Departamento de Engenharia Química, Instituto Superior de Engenharia de Lisboa, Instituto Politécnico de Lisboa, R. Conselheiro Emídio Navarro, 1, 1959-007 Lisboa, Portugal

<sup>f</sup>Centro de Química Estrutural, Institute of Molecular Sciences, Instituto Superior Técnico, Universidade de Lisboa, Av. Rovisco Pais, 1049-001 Lisboa, Portugal.

E-mail: pombeiro@ist.utl.pt

† Electronic supplementary information (ESI) available: Details of X-ray diffraction and synthetic and catalytic studies. CCDC 2353189. For ESI and crystallographic data in CIF or other electronic format see DOI: <https://doi.org/10.1039/d4nr02298j>

The presence of VOCs in the atmosphere has raised significant concerns due to their harmful effects on human health and the environment. Current VOC mitigation strategies involve either their replacement by safer compounds or treating them before atmospheric release. Thermal oxidation converts these compounds into carbon dioxide and water, significantly reducing pollution, although it is energy-intensive and less effective for low VOC concentrations.<sup>18</sup> Recently, diverse technologies have been explored to eliminate VOCs.<sup>18</sup> Among them, partial and selective catalytic oxidation is particularly promising due to high VOC conversion rates and the formation of high-value products such as benzyl alcohol, benzaldehyde, and benzoic acid which are crucial intermediates in various industries. BTEX compounds—benzene, toluene, ethylbenzene, and xylene—pose significant risks. Toluene is a prominent pollutant, and in the industrial oxidation of toluene, various catalytic processes are employed to achieve efficient conversion. One widely used method involves thermal catalytic oxidation, where toluene is oxidized over noble metal catalysts such as platinum (Pt) and palladium (Pd) supported on different substrates. This process is effective at high temperatures, typically 200 to 600 °C, and results in the formation of CO<sub>2</sub> and H<sub>2</sub>O.<sup>19</sup> Moreover, several technologies, such as thermal or non-thermal catalytic oxidation,<sup>20</sup> adsorption,<sup>21</sup> photocatalytic oxidation,<sup>22</sup> and plasma thermal catalysis,<sup>23</sup> have been deployed for the mitigation of the problem. Catalytic oxidation is highly effective for toluene removal, but its success depends on the reaction conditions and catalyst performance.<sup>24</sup>

Common catalysts for oxidative conversion include noble metals, other transition metals, metal–organic frameworks (MOFs),<sup>25</sup> perovskite catalysts,<sup>26</sup> and spinel-based catalysts.<sup>27</sup> Noble metals are efficient but costly and sensitive to chloride poisoning<sup>28</sup> whereas non-noble transition metal oxides<sup>29</sup> and composite oxides<sup>30</sup> can be more cost-effective and perform well.

Recent research has concentrated on developing novel catalysts that combine noble metal nanoparticles (such as Pd, Pt, Au, Ru, and Ag) with various materials and metal oxide-based catalysts (like Co, Mn, Ce, Al, La, Zn, Ni, and Cu) to enhance environmental catalytic reactions, especially for the oxidation of toluene.<sup>31</sup>

Moreover, supported noble metal alloys, prepared by adding a second noble metal, have demonstrated superior performance in toluene oxidation.<sup>32</sup>

Doping precious metals like Pt, Pd, Au, and Ru in VOC catalytic combustion has revealed synergistic effects, attributed to electronic or geometric changes.<sup>33</sup>

In this study, the catalytic performance of a metallasilsesquioxane/phosphazene compound was examined, to our knowledge for the first time, for the oxidation of VOCs, with toluene serving as a model substrate due to its widespread use in industrial applications and its prevalence as an environmental pollutant.

## Results and discussion

For the method of synthesis, a three-step reaction was chosen. First, reactive siloxanolate [PhSi(O)Na]<sub>n</sub> species were *in situ* prepared *via* alkaline hydrolysis<sup>34</sup> of PhSi(OMe)<sub>3</sub> assisted by the action of NaOH in ethanol solution. Second, an exchange reaction with CuCl<sub>2</sub> was used for the formation of {[PhSiO<sub>2</sub>]<sub>x</sub>[Cu]<sub>y</sub>[Na]<sub>z</sub>} species. In the third stage, the *in situ* prepared {[PhSiO<sub>2</sub>]<sub>x</sub>[Cu]<sub>y</sub>[Na]<sub>z</sub>} intermediate was reacted with bis(triphenylphosphine)iminium chloride (PPNCl). Very recently, we observed that such copper–sodium silsesquioxanes are structurally flexible upon complexation with organic ligands.<sup>35</sup> Indeed, as a result of the synthetic procedure (Scheme S1<sup>†</sup>), intriguing ionic complex [(PPN)<sup>+</sup>]<sub>2</sub> Cu<sub>9</sub>Na<sub>4</sub>[(Ph<sub>6</sub>Si<sub>6</sub>O<sub>12</sub>)<sub>2</sub>-(Ph<sub>4</sub>Si<sub>4</sub>O<sub>9</sub>)<sub>2</sub>]<sup>2-</sup> · 3.5EtOH **1** has been isolated in 69% yield (Fig. 1). Complex **1** (Fig. 1, top) exhibits several unusual (for CLMSSs) structural features. First of all, compound **1** is the very first observation of the metallasilsesquioxane/phosphazene complex. In turn, the cage component of complex **1** included an unusual set of silsesquioxane ligands: two pairs of Si<sub>6</sub>-cyclic and Si<sub>4</sub>-acyclic ones (Fig. 1, bottom left). This allows the formation of an intriguing metal oxide core of Cu<sub>9</sub><sup>II</sup>Na<sub>4</sub><sup>I</sup> nuclearity (Fig. 1, bottom right). In sum, it provides 22 positive charges, which could not be compensated by 24 negative charges from four silsesquioxane ligands (two (Ph<sub>6</sub>Si<sub>6</sub>O<sub>12</sub>)<sup>6-</sup> cycles and two (Ph<sub>4</sub>Si<sub>4</sub>O<sub>9</sub>)<sup>6-</sup> acyclic species). Due to the presence of two external PPN<sup>+</sup> cations, the whole complex **1** is electrobalanced with central cage copper–sodium silsesquioxane playing the role of an unusual dianionic component.

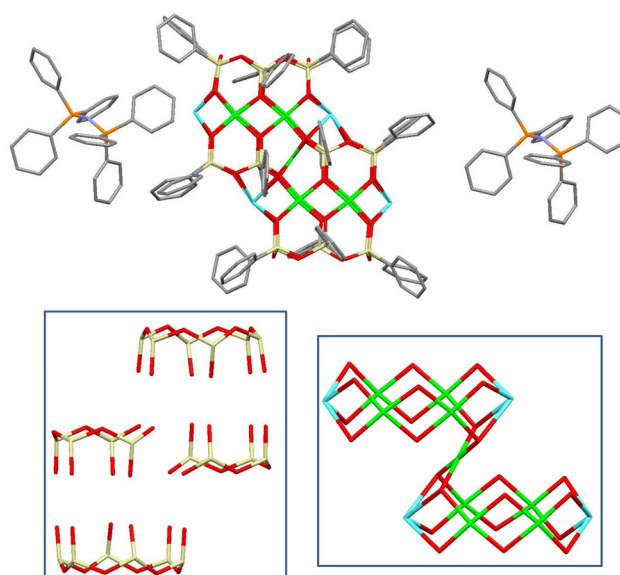


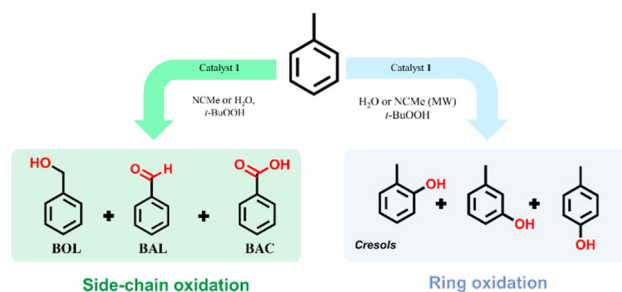
**Fig. 1** Top: Molecular structure of copper–sodium phenylsilsesquioxane/bis(triphenylphosphine)iminium complex **1**. Bottom left: Structures of two pairs of (Si<sub>6</sub> cyclic and Si<sub>4</sub> acyclic) ligands in **1**. Bottom right: Cu<sub>9</sub>Na<sub>4</sub> metal core in **1**. Color code: Si, yellow; O, red; Cu, green; Na, aqua; P, orange; and C, gray. Hydrogen atoms are omitted for clarity.

In more detail, the type of molecular structure represents a “fusion” of two  $\text{Cu}_4\text{Na}_2$ -based fragments *via* the central ninth copper ion. One can see that these  $\text{Cu}_4\text{Na}_2$ -based fragments (Fig. 2 top) are distorted sandwich architectures (similar to  $\text{Si}_{12}$ -based potassiumcopper<sup>36</sup> or rubidiumcopper<sup>4b</sup> silsesquioxane cages). An absence of two silicon atoms in “unfinished”  $\text{Si}_{10}\text{Cu}_4\text{Na}_2$ -units allowed them to be connected through the central copper ion as a pivot point. It is intriguing that the resulting cage nevertheless represents some flexibility in its geometry, *e.g.* the opposite  $\text{Na}\cdots\text{Na}$  distances are not the same (8.117 Å *vs.* 8.205 Å).

In general, the idealized symmetry of the cage-like dianion is  $C2h(2/m)$ . However, in the crystal, due to the crystal packing effects complex **1** possesses the intrinsic symmetry  $C1$  (**1**). The coordination environment of all copper cations is a planar square. The sodium cations can be divided into “external” (Na2 and Na4) having the tetragonal-pyramidal coordination and “internal” (Na1 and Na3) adopting the distorted mono-capped octahedral coordination (see the ESI†).

### Peroxidative oxidation of toluene

Complex **1** was explored as a catalyst for the peroxidative oxidation of toluene, as illustrated in Scheme 1.



**Scheme 1** Peroxidative oxidation of toluene catalyzed by **1**. TOL – toluene; BOL – benzyl alcohol; BAL – benzaldehyde; BAC – benzoic acid; MW – microwave irradiation.

In this study, *tert*-butyl hydroperoxide (*t*-BuOOH) (aq. 70% was used as its source) was chosen as the oxidant as it is known to be highly effective in various oxidation reactions, as well as compatible with a wide range of metal catalysts, including those based on copper, which makes it a very versatile oxidant. *t*-BuOOH is relatively stable at higher temperatures compared to other peroxides, namely hydrogen peroxide (also known as an environmentally friendly oxidant); it is soluble in both organic solvents and water, making it possible to include more environmentally friendly solvents.<sup>37–40</sup> Acetonitrile is always our first choice as an organic solvent because it is very stable, does not undergo unwanted reactions under oxidising conditions, is compatible with a wide range of oxidants and catalysts and has a high dielectric constant, making it an excellent solvent for polar reactions, which often include oxidation processes.<sup>41</sup>

As shown above, **1** demonstrates a nontrivial combination of two pairs of  $\text{Si}_6$ -cyclic/ $\text{Si}_4$ -acyclic silsesquioxane ligands and a fusion of two  $\text{Si}_{10}\text{Cu}_4\text{Na}_2$  fragments, combined *via* the central ninth copper ion. At first glance, a high catalytic activity can be predicted for this complex because its molecule has nine potentially active metal centres.

Copper's remarkable catalytic capabilities have been showcased across a range of oxidation reactions, namely arising from its capacity to participate readily in redox processes due to its easily variable oxidation states, notably  $\text{Cu(I)}$  and  $\text{Cu(II)}$ .<sup>40,42</sup> These oxidation states are expected to play a pivotal role in catalyzing the oxidation of organic substances such as toluene. The cage-like structure, on the other hand, can prevent substrate molecules from easily accessing these active centres, potentially affecting the overall catalytic efficiency. In addition, the complex shows low solubility in the solvents tested, acetonitrile and water, which can give a heterogeneous characteristic to the catalytic system, which can lead to lower yields, but with the advantage of allowing the catalyst to be recovered and reused. During this study, several parameters were investigated, including the catalyst amount, reaction time, effect of an acid additive, heterogeneity of the catalytic system, microwave irradiation as an alternative energy input, amount of oxidant, and temperature. Our standard conditions involved a temperature of 80 °C and a reaction time of

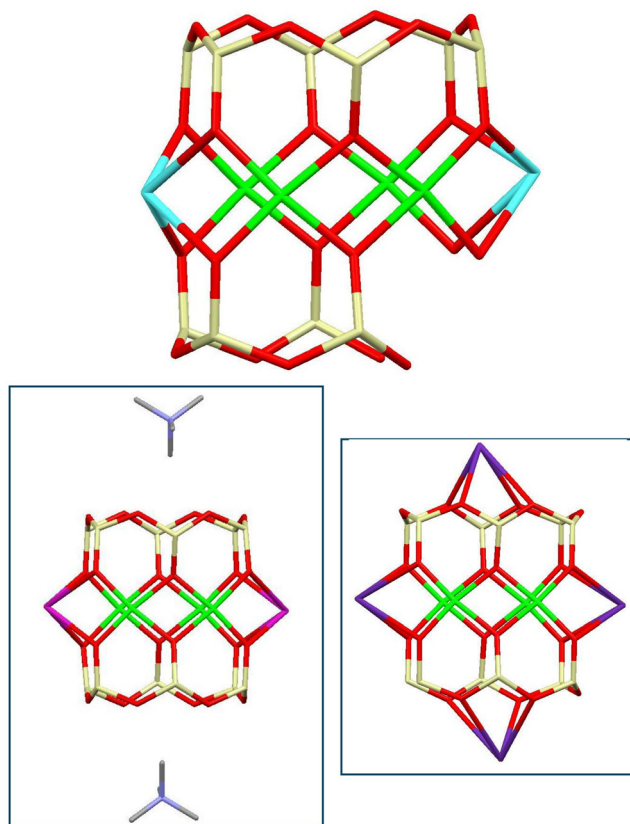


**Fig. 2** Top: Molecular structure of the unfinished  $\text{Si}_{10}\text{Cu}_4\text{Na}_2$ -sandwich fragment of **1**. Bottom left:  $\text{Si}_{12}\text{Cu}_4\text{K}_2$ -based compound from ref. 35. Bottom right:  $\text{Si}_{12}\text{Cu}_4\text{Rb}_4$ -based compound from ref. 4b.

24 hours. The oxidation of toluene was evaluated both without a catalyst and under typical reaction conditions. No significant products were detected without a catalyst, underscoring its essential role. Similarly, the presence of the oxidant was crucial, as in its absence no oxidation products were observed.

The catalytic studies started with the examination of the catalyst loading effect, conducting the reactions with 0.5 mmol of toluene and 1 mmol (2 equiv.) of *t*-BuOOH oxidant in 0.3 mL of acetonitrile at 80 °C, without any additives for 24 hours. It was observed that increasing the catalyst amount from 0.2 to 1 mol% did not significantly increase the total reaction yield, with a very slight decrease noted at 0.4 mol% (Fig. 3a and Table 1, entries 1–3). Considering the limited solubility of the catalyst and the small reaction volume, the addition of more catalysts may hinder substrate diffusion, thereby reducing access to the metal centers. Therefore, to make better use of the catalyst, the remaining studies were

carried out with the lowest catalyst loading, 0.2 mol%, for toluene oxidation. Typical reactions were carried out with a 1 : 2 excess of oxidant relative to the substrate. Tests with proportions of 1 : 1 and 1 : 4 were conducted to understand the effect of the amount of oxidant (Fig. 3b and Table 1, entries 10 and 11). Using a smaller amount of TBHP (equimolar with the substrate) resulted in a significant drop in the total yield, especially for the more oxidized products, benzaldehyde and benzoic acid, whereas the total yield of the less oxidized product (benzyl alcohol) increased significantly (around six times more). Increasing the oxidant concentration to a 1 : 4 molar ratio only led to a slight total yield increase of about 3%, but the product distribution shifted, with a much greater quantity of acid being produced compared to the other products. Regardless of the amount of oxidant, benzoic acid was always the major product, showing that the oxidation of toluene in the presence of catalyst **1** is considerably selective for the acid.

The addition method of the oxidant was investigated by comparing the effect of its entire addition at the beginning of the reaction with that of the addition of the same volume but sequentially. Thus, we repeated the conditions of assay 7, a reaction conducted for 6 h at 80 °C, but with the oxidant being added in small volumes every hour (Table 1, entry 13). Effectively, sequential addition resulted in a higher total yield, 33.6% (Table 1, entry 13), compared to 21.7% (Table 1, entry 7). Another intriguing observation was the presence of a substantially larger amount of benzyl alcohol, indeed the highest value recorded throughout the catalytic study. Nevertheless, benzoic acid remained the predominant product.

To investigate the influence of reaction time on both yield and selectivity in the peroxidative oxidation of toluene, experiments were carried out at 1, 3, 6, 24, and 48 h (Fig. 4a). Increasing the reaction time from 1 to 24 h significantly enhanced the formation of more oxygenated products, particularly the aldehyde and even more the acid, especially with prolonged reaction times. Notably, no alcohol was observed after the longest reaction periods. The total yield improved from a modest 3.6% after 1 h (Table 1, entry 5) to 24.8% after 24 h (Table 1, entry 1). This increase in yield was accompanied by a substantial rise in the selectivity for benzoic acid, which increased from 31% to 65% (Table 1, entries 5 and 1, respectively). Extending the reaction time beyond 24 h (48 h in total) resulted in a modest increase in yield to 26.2%, but with a more marked selectivity for benzoic acid of 73% (Table 1, entry 8).

Temperature has a high impact on the conversion rate of toluene. At 30 °C, the conversion into the oxidized products was barely above 1%, while increasing the temperature to 50 °C raised it to nearly 7% (Fig. 4b and Table 1, entries 14 and 15). However, these results remain modest compared to those achieved at 80 °C (Fig. 4b and Table 1, entry 1). This outcome is expected given the relatively high stability of the C–H bond in hydrocarbons such as toluene. Higher temperatures provide the necessary thermal energy to overcome the activation energy barrier for bond dissociation. Additionally, cata-

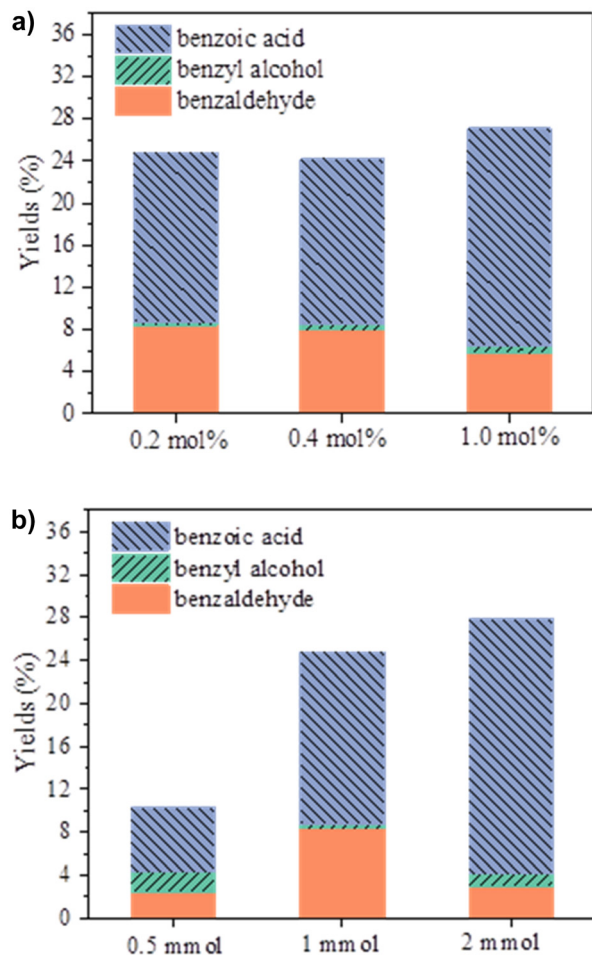


**Fig. 3** (a) Influence of catalyst loading (mol% based on toluene) on the yield and selectivity. Reaction conditions: toluene (0.5 mmol), *t*-BuOOH (1 mmol), 80 °C, 24 h. (b) Influence of the amount of oxidant on the yield and selectivity. Reaction conditions: 1  $\mu$ mol of **1** (0.2 mol%), toluene (0.5 mmol), 80 °C, 24 h. BOL – benzyl alcohol; BAL – benzaldehyde; and BAC – benzoic acid.



**Table 1** Peroxidative oxidation of toluene with *t*-BuOOH as the oxidant and using **1** as the catalyst<sup>a</sup>

Entry	Reaction time (h)	Solvent	$n_{\text{acid}}/n_{\text{cat}}$	Yield <sup>b</sup> (%)				
				Cresols	BAL	BOL	BAC	Total
1	24	NCMe	—	n.d.	8.4	0.3	16.1	24.8
2 <sup>c</sup>	24	NCMe	—	n.d.	8.0	0.5	15.7	24.2
3 <sup>d</sup>	24	NCMe	—	n.d.	5.8	0.6	20.7	27.1
4	24	H <sub>2</sub> O	—	1.3	1.0	n.d.	6.7	9.0
5	1	NCMe	—	n.d.	1.8	0.6	1.2	3.6
6	3	NCMe	—	n.d.	2.5	0.7	3.6	6.8
7	6	NCMe	—	n.d.	6.3	1.1	14.3	21.7
8	48	NCMe	—	n.d.	7.1	n.d.	19.1	26.2
9	24	NCMe	5	n.d.	5.3	n.d.	22.0	27.3
10 <sup>e</sup>	24	NCMe	—	n.d.	2.5	1.8	6.0	10.3
11 <sup>f</sup>	24	NCMe	—	n.d.	3.0	1.1	23.7	27.8
12 <sup>g</sup>	24	NCMe	—	n.d.	6.8	n.d.	10.1	16.9
13 <sup>h</sup>	24	NCMe	—	n.d.	6.6	4.6	22.4	33.6
14 <sup>i</sup>	24	NCMe	—	n.d.	0.4	0.3	0.6	1.3
15 <sup>j</sup>	24	NCMe	—	n.d.	2.7	3.5	0.5	6.7
16 <sup>k</sup>	24	NCMe	—	n.d.	5.8	0.2	14.1	20.1
17	24	H <sub>2</sub> O	5	0.2	7.7	n.d.	9.5	17.4
18	24	H <sub>2</sub> O	50	0.8	6.2	1.8	28.5	37.5
19	24	H <sub>2</sub> O	100	0.4	n.d.	n.d.	39.9	40.3
20 <sup>l</sup>	0.5	NCMe	—	1.5	3.6	1.3	0.3	6.7
21 <sup>l</sup>	1.5	NCMe	—	1.9	4.8	n.d.	0.6	7.3
22 <sup>l</sup>	0.5	H <sub>2</sub> O	—	0.7	4.1	n.d.	1.3	6.1

<sup>a</sup> Reaction conditions: catalyst (1  $\mu\text{mol}$ ; 0.2 mol%), toluene (0.5 mmol), *t*-BuOOH (1 mmol), water or acetonitrile (0.3 mL), 80 °C, 24 h. BAL – benzaldehyde; BOL – benzyl alcohol; BAC – benzoic acid; n.d. – not detected. <sup>b</sup> Molar yield (%) based on the substrate, *i.e.* moles of product (cresols, benzaldehyde, benzyl alcohol or benzoic acid) per 100 mol of toluene, determined by GC, using the internal standard method. <sup>c</sup> 0.4 mol% of catalyst. <sup>d</sup> 1 mol% of catalyst. <sup>e</sup> 0.5 mmol of *t*-BuOOH (1 : 1). <sup>f</sup> 2 mmol of *t*-BuOOH (1 : 4). <sup>g</sup> Separation of the catalyst after 6 h and continuation of the reaction until completing 24 h. <sup>h</sup> Addition of the oxidant sequentially, approximately 0.15 mmol h<sup>-1</sup> over the course of the 6 h reaction. <sup>i</sup> Reaction performed at 30 °C. <sup>j</sup> Reaction performed at 50 °C. <sup>k</sup> 2nd cycle. <sup>l</sup> Under MW irradiation (10 W).

lysts often become more active at elevated temperatures, offering more active sites for the reaction.<sup>42</sup>

Despite the advantages of using acetonitrile as the solvent, the search for environmentally sustainable systems led us to test water as an alternative. The reaction in water resulted in a lower total yield (9%) (Table 1, entry 4) compared to 24.8% in acetonitrile (Table 1, entry 1) under the same conditions (24 h at 80 °C). Moreover, there are other notable differences. The reaction in water favored the formation of cresols, accounting for 14% of the total yield, which was not observed in acetonitrile. Additionally, we investigated the effect of adding an acid additive (Fig. 5). Using a nitric acid-to-catalyst ratio of 5, the total yield in acetonitrile increased slightly from 24.8 (in the absence of HNO<sub>3</sub>) (Fig. 5 and Table 1, entry 1) to 27.3% (in the presence of HNO<sub>3</sub>) (Fig. 5 and Table 1, entry 9), respectively. Interestingly, when the same amount of acid was used in the reaction in water, the total yield increased significantly from 9% (in the absence of HNO<sub>3</sub>) (Fig. 5 and Table 1, entry 4) to 17.4% (in the presence of HNO<sub>3</sub>) (Fig. 5 and Table 1, entry 17). In both cases, the increase was mainly due to a higher production of benzoic acid. These results motivated us to explore the effect of the acid additive in water further, testing ratios of 50 : 1 and 100 : 1. In these cases, the positive effect was even more pronounced, with the total yield rising to 37.5% (50 : 1) (Fig. 5 and Table 1, entry 18) and 40.3% (100 : 1) (Fig. 5 and Table 1, entry 19), mainly due to an increased production of benzoic acid. In the latter case, benzoic acid was almost the

sole product at 39.9%, with only a small amount of cresol (0.4%) breaking its exclusivity.

The promoting effect of adding an acid additive aligns with observations from other catalytic systems,<sup>43</sup> although in this study, the effect is more pronounced in the presence of water. The acidic environment created by HNO<sub>3</sub> in water can lead to a greater activation of the catalyst, improving its ability to facilitate the oxidation process. This may involve the protonation of the catalyst (*e.g.*, ligand protonation with the generation of vacant coordination positions) or the formation of other more reactive catalytic species.<sup>44,45</sup> In acetonitrile, these effects are less pronounced because the solvent already provides an optimal environment for the reaction.

To exploit the advantages of heterogeneous catalysts such as selectivity and reuse, we investigated the heterogeneous nature of **1**, and a hot filtration test was performed (Table 1, entry 12).<sup>38–40,46</sup> The catalytic reaction was carried out under the standard conditions for 6 h, whereafter the catalyst was removed by hot filtration and the supernatant was kept under the same conditions for the full 24 h period (Table 1, entry 12). The results were compared with those obtained after 6 h (Table 1, entry 7) and 24 h (Table 1, entry 1) in the presence of the catalyst. The 24 h yield obtained upon removing the catalyst after 6 h (16.9%, entry 12) was much lower than that obtained in its presence (24.8%, Table 1, entry 1) and was not higher than that after 6 h (21.7%, Table 1, entry 7), thus suggesting a suppression of catalytic activity upon solid

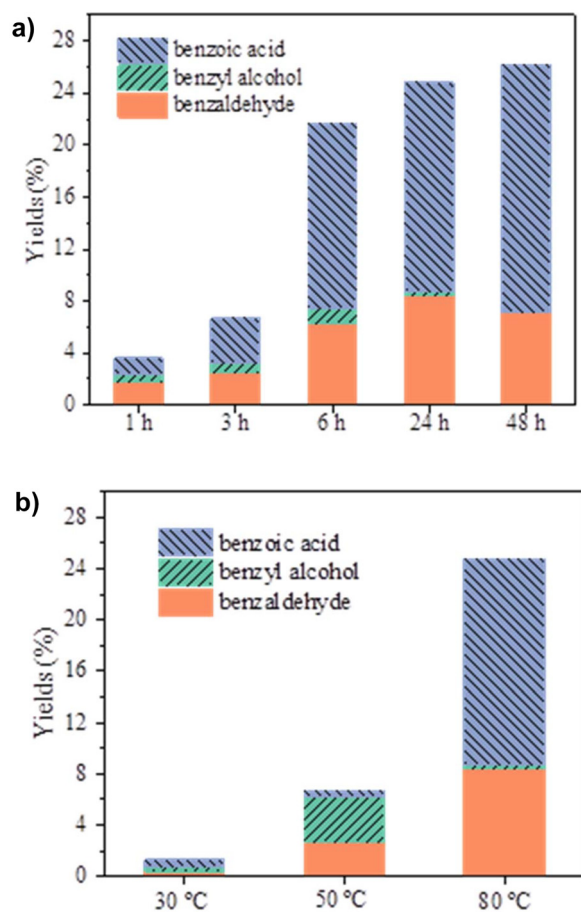


**Fig. 4** (a) Influence of the reaction time on the yield and selectivity. Reaction conditions: 1  $\mu\text{mol}$  of **1** (0.2 mol%), toluene (0.5 mmol), TBHP (1 mmol), 80 °C, 1–48 h. (b) Influence of the reaction temperature on the yield and selectivity. Reaction conditions: 1  $\mu\text{mol}$  of **1**, toluene (0.5 mmol), TBHP (1 mmol), 24 h. BOL – benzyl alcohol; BAL – benzaldehyde; and BAC – benzoic acid.

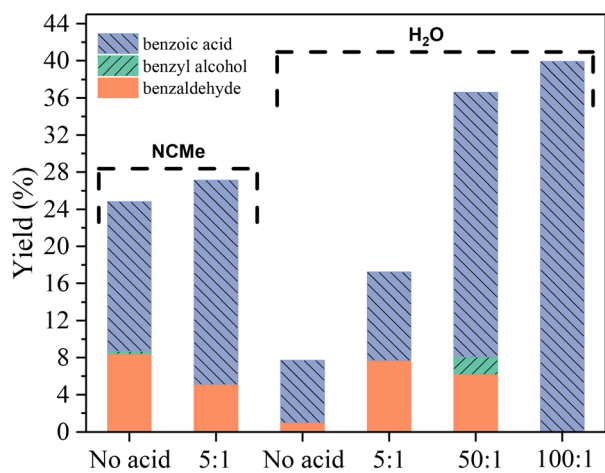


**Fig. 5** Influence of the acid additive on the yield and selectivity for the oxidation of the methyl group in toluene. Reaction conditions: 1  $\mu\text{mol}$  of **1** (0.2 mol%), toluene (0.5 mmol), TBHP (1 mmol), NcMe or H<sub>2</sub>O, nitric acid ( $n_{\text{acid}}/n_{\text{cat}} = 0, 5, 50$  or 100), 80 °C. BOL – benzyl alcohol; BAL – benzaldehyde; and BAC – benzoic acid.

catalyst removal and substantiating a heterogeneous behaviour of the catalyst. However, at the end of the reactions, although a catalyst deposit is visible, the reaction solution exhibits a blue coloration typical of a copper compound, indicating that catalyst solubility has occurred to a limited extent, but (see above) forming an inactive dissolved species.

The recyclability of **1** was evaluated for another cycle after 24 h of reaction. To achieve this, the solid catalyst was isolated by filtration after the first catalytic cycle and thoroughly washed with 10 mL of NcMe. The isolated catalyst was then dried for a minimum of 15 h at 68 °C before being reintroduced for reuse under identical reaction conditions. In this second cycle, we observed a decline of approximately 19% in its catalytic activity compared to the first cycle, although maintaining the same distribution of products. This behaviour can be accounted for by the decrease of the solid catalyst load in view of its decomposition, to some extent, into an inactive soluble species (see above).

The catalytic performance of compound **1** was also evaluated under microwave radiation (MW) in acetonitrile and water. The objective was to evaluate the possibility of converting toluene in a short period. Indeed, it was found that when the reaction was conducted under MW radiation at 80 °C, a total yield of 6.3% was achieved in 0.5 h in acetonitrile (Table 1, entry 20), a value identical to the 6.5% obtained after 3 h when the reaction occurred at the same temperature using conventional heating (Table 1, entry 6). However, unlike the catalytic studies performed with conventional heating, MW radiation seems to promote the oxidation of the aromatic ring, making the reaction less selective. In the case of the reaction carried out in water, the acceleration is more pronounced, as the total yield of 7.3% obtained after 0.5 h (Table 1, entry 22) is not much lower than the 9% yield obtained after 24 h of conventional heating (Table 1, entry 4).

It is known that the peroxidative oxidation of toluene can occur both at the methyl group (side-chain oxidation) and at the aromatic ring (ring oxidation).<sup>16d,18a,47</sup> In our study, the oxidation of the methyl group is markedly prominent, leading to the formation of benzyl alcohol, benzaldehyde and benzoic acid, while the oxidation of the aromatic ring occurs in reactions carried out in water or when using MW radiation as an alternative energy input. The C–H bonds in the methyl group are weaker and less stable compared to the aromatic C–H bonds, making them generally easier to activate. Ring oxidation is more difficult to achieve due to the high stability and delocalized nature of the aromatic ring, which requires higher activation energy.<sup>16d,47</sup>

To demonstrate the radical mechanism of toluene oxidation, diphenylamine (Ph<sub>2</sub>NH) was used as a radical scavenger in a stoichiometric amount relative to *t*-BuOOH. This significantly inhibited the oxidation of toluene when catalyst **1** was present, suggesting a radical pathway. The expected mechanism possibly involves a branched chain process initiated by the activation of TBHP by copper complex **1**. This activation leads to the formation of *tert*-butylperoxyl (*t*-BuOO<sup>•</sup>) and *tert*-butoxyl (*t*-BuO<sup>•</sup>) radicals *via* the reduction of Cu(II)

and the oxidation of Cu(I), respectively. Initially, the *t*-BuO<sup>•</sup> radical abstracts a hydrogen atom from toluene, generating a benzyl radical (PhCH<sub>2</sub><sup>•</sup>). This benzyl radical then reacts with molecular oxygen (O<sub>2</sub>) to form a benzyl peroxy radical (PhCH<sub>2</sub>OO<sup>•</sup>). This benzyl peroxy radical undergoes disproportionation, producing benzyl alcohol and benzaldehyde. Benzaldehyde can also result from the metal-catalyzed oxidation of benzyl alcohol. Additionally, the benzyl peroxy radical (PhCH<sub>2</sub>OO<sup>•</sup>) can abstract a hydrogen atom from toluene, regenerating the benzyl radical and forming benzyl hydroperoxide, which subsequently oxidizes to yield benzoic acid in the presence of the catalyst. Further chain branching occurs when benzyl hydroperoxide generates new oxygen-based radicals.<sup>48</sup>

Complex **1** appears as a promising catalyst for the peroxidative oxidation of toluene with a total conversion to the oxidized products of 24.8% over 24 h at 80 °C without any additives. For example, the catalyst exhibits a higher activity than the copper compound [Cu<sub>2</sub>(μ-1kONO':2kOO':3kO-HL)(μ-1kONO':2kOO'-HL)]<sub>2</sub>·4DMF [H<sub>3</sub>L = (2,3-dihydroxybenzylidene)-2-hydroxybenzohydrazide] with a total conversion of 10.7% in 3 h at 80 °C, despite the addition of HNO<sub>3</sub>.<sup>49</sup> Other copper-based catalysts, such as [Cu(tyr)<sub>2</sub>]<sub>n</sub> (tyr = L-tyrosinato) (with a total conversion of 42.0% in 4 h, at 60 °C, with the addition of NaHCO<sub>3</sub>) or Fe<sub>3</sub>O<sub>4</sub>@SiO<sub>2</sub>/CPTMS/[Cu(tyr)<sub>2</sub>]<sub>n</sub> [tyr = L-tyrosinato; CPTMS = 3-(chloropropyl) trimethoxysilane] (with a total conversion of 30.0% in 2 h, at 60 °C, with the addition of NaHCO<sub>3</sub>)<sup>49</sup> and [Cu(HL)Cl(CH<sub>3</sub>OH)] [H<sub>2</sub>L = 2-hydroxy(2-hydroxybenzylidene) benzohydrazide] (with a total conversion of 38.7% in 1 h, at 60 °C, under MW irradiation),<sup>30</sup> demonstrate a higher catalytic efficiency under varying conditions, some achieving higher conversions in significantly shorter times and lower temperatures, often with the aid of additives or MW irradiation.<sup>50</sup> Nevertheless, it is worth noting that the maximum yield obtained for **1** was 40.3% in water in the presence of an acidic additive.

## Conclusions

A convenient self-assembly of copper–sodium silsesquioxane in the presence of bis(triphenylphosphine)iminium chloride led to an unprecedented metallasilsesquioxane/phosphazene compound **1**. This compound features a unique ionic structure with a Cu<sub>9</sub>Na<sub>4</sub>-silsesquioxane cage as a dianion and two external PPN<sup>+</sup> cations, showcasing a specific connection of two Cu<sub>4</sub>Na<sub>2</sub>-sandwich fragments *via* a central copper center.

The catalytic performance of **1** was evaluated through the peroxidative oxidation of toluene using *tert*-butyl hydroperoxide (*t*-BuOOH). The primary oxidation products were benzaldehyde (BAL), benzyl alcohol (BOL), and benzoic acid (BAC), with benzoic acid generally being predominant. The highest total yield in acetonitrile (NCMe) was 33.6% without any additive, while in water, it reached 40.3% with an acidic additive at 80 °C. The presence of cresols was observed only in water and under microwave irradiation in NCMe. Higher *t*-BuOOH con-

centrations and sequential addition of the oxidant improved the total yield, favoring more oxidized products such as benzoic acid.

The copper–sodium silsesquioxane complex offers high catalytic efficiency and significant product yields. Its unique ionic structure introduces a novel metallasilsesquioxane/phosphazene compound, paving the way for advancements in the field. The catalyst's versatility under different reaction conditions allows fine-tuning for optimal yields and selectivity, indicating its potential for industrial-scale oxidation applications. Nevertheless, the decomposition of the catalyst, although to a limited extent, into an inactive soluble species hampers its effective recycling.

Moreover, the multi-step synthesis and precise conditions may limit scalability. Additionally, its performance depends on specific reaction conditions, complicating optimization. While it is effective for toluene oxidation, further exploration is needed for other substrates.

Overall, the copper–sodium silsesquioxane complex shows promise as a toluene oxidation catalyst due to its high efficiency, structural novelty, and tunable reaction conditions, opening new research avenues in metallasilsesquioxane chemistry.

## Data availability

Crystallographic data for compound **1** have been deposited at the CCDC (2353189).†

## Conflicts of interest

There are no conflicts to declare.

## Acknowledgements

We are grateful for the financial support from the Russian Science Foundation (RSF grant 22-13-00250, synthesis). This work (elemental analysis) was in part supported by the Ministry of Science and Higher Education of the Russian Federation (Contract No. 075-03-2023-642) and was performed employing the equipment of the Center for Molecular Composition Studies of INEOS RAS. We thank FCT for 2022.02069.PTDC (<https://doi.org/10.54499/2022.02069.PTDC>), UIDB/00100/2020 (<https://doi.org/10.54499/UIDB/00100/2020>) and UIDP/00100/2020 (<https://doi.org/10.54499/UIDP/00100/2020>) projects of Centro de Química Estrutural, and LA/P/0056/2020 (<https://doi.org/10.54499/LA/P/0056/2020>) of the Institute of Molecular Sciences. We are also grateful to Instituto Politécnico de Lisboa for the IPL/IDI&CA2023/SMARTCAT\_ISEL project.

## References

- M. M. Levitsky, Y. V. Zubavichus, A. A. Korlyukov, V. N. Khrustalev, E. S. Shubina and A. N. Bilyachenko, *J. Cluster Sci.*, 2019, **30**, 1283 and references cited therein.
- (a) M. M. Levitsky, A. N. Bilyachenko, E. S. Shubina, J. Long, Y. Guari and J. Larionova, *Coord. Chem. Rev.*, 2019, **398**, 213015; (b) Y.-N. Liu, J.-L. Hou, Z. Wang, R. K. Gupta, Z. Jagličić, M. Jagodič, W.-G. Wang, C.-H. Tung and D. Sun, *Inorg. Chem.*, 2020, **59**, 5683; (c) A. N. Kulakova, K. Nigoghossian, G. Félix, V. N. Khrustalev, E. S. Shubina, J. Long, Y. Guari, L. D. Carlos, A. N. Bilyachenko and J. Larionova, *Eur. J. Inorg. Chem.*, 2021, 2696; (d) G. Félix, S. Sene, A. N. Kulakova, A. N. Bilyachenko, V. N. Khrustalev, E. S. Shubina, Y. Guari and J. Larionova, *RSC Adv.*, 2023, **13**, 26302; (e) M. Tricoire, N. Jori, F. F. Tirani, R. Scopelliti, I. Zivković, L. S. Natrajan and M. Mazzanti, *Chem. Commun.*, 2024, **60**, 55.
- (a) K. Nigoghossian, A. N. Kulakova, G. Félix, V. N. Khrustalev, E. S. Shubina, J. Long, Y. Guari, S. Sene, L. D. Carlos, A. N. Bilyachenko and J. Larionova, *RSC Adv.*, 2021, **11**, 34735; (b) K. Sheng, W.-D. Si, R. Wang, W.-Z. Wang, J. Dou, Z.-Y. Gao, L.-K. Wang, C.-H. Tung and D. Sun, *Chem. Mater.*, 2022, **34**, 4186; (c) S. Marchesi, C. Bisio and F. Carniato, *Processes*, 2022, **10**(4), 758; (d) G. Félix, A. N. Kulakova, S. Sene, V. N. Khrustalev, M. A. Hernández-Rodríguez, E. S. Shubina, T. Pelluau, L. D. Carlos, Y. Guari, A. N. Carneiro Neto, A. N. Bilyachenko and J. Larionova, *Front. Chem.*, 2024, **12**, 1379587.
- (a) H. Chun and D. Moon, *J. Am. Chem. Soc.*, 2023, **145**, 18598; (b) A. N. Bilyachenko, I. S. Arteev, V. N. Khrustalev, L. S. Shul'pina, A. A. Korlyukov, N. S. Ikonnikov, E. S. Shubina, Y. N. Kozlov, N. R. Conceição, M. F. C. G. da Silva, K. T. Mahmudov and A. J. L. Pombeiro, *Inorg. Chem.*, 2023, **62**, 13573; (c) A. N. Bilyachenko, G. S. Astakhov, A. N. Kulakova, A. A. Korlyukov, Y. V. Zubavichus, P. V. Dorovatovskii, L. S. Shul'pina, E. S. Shubina, N. S. Ikonnikov, M. V. Kirillova, A. Y. Zueva, A. M. Kirillov and G. B. Shul'pin, *Cryst. Growth Des.*, 2022, **22**, 2146.
- K. Sheng, R. Wang, X. Tang, M. Jagodič, Z. Jagličić, L. Pang, J.-M. Dou, Z.-Y. Gao, H.-Y. Feng, C.-H. Tung and D. Sun, *Inorg. Chem.*, 2021, **60**, 14866.
- K. Sheng, Y.-N. Liu, R. K. Gupta, M. Kurmoo and D. Sun, *Sci. China: Chem.*, 2021, **64**, 419.
- A. N. Bilyachenko, E. I. Gutsul, V. N. Khrustalev, O. Chusova, P. V. Dorovatovskii, V. A. Aliyeva, A. B. Paninho, A. V. M. Nunes, K. T. Mahmudov, E. S. Shubina and A. J. L. Pombeiro, *Inorg. Chem.*, 2023, **62**, 15537.
- P. Loganathan, R. S. Pillai, V. Jeevananthan, E. David, N. Palanisami, N. S. P. Bhuvanesh and S. Shanmugan, *New J. Chem.*, 2021, **45**, 20144.
- (a) S. Marchesi, C. Bisio, F. Carniato and E. Boccaleri, *Inorganics*, 2023, **11**, 426; (b) L. Qiao, W. Zhang and R. Yang, *Eur. Polym. J.*, 2024, **211**, 113027.
- (a) A. R. Willauer, A. M. Dabrowska, R. Scopelliti and M. Mazzanti, *Chem. Commun.*, 2020, **56**, 8936; (b) M. R. Gau and M. J. Zdilla, *Inorg. Chem.*, 2021, **60**, 286.
- A. N. Bilyachenko, N. Reis Conceição, M. F. C. Guedes da Silva, K. T. Mahmudov, G. B. Shul'pin and A. J. L. Pombeiro, *Synthesis, Structure and Catalytic Application of Cage Metallasilsesquioxanes in Synthesis and Applications in Chemistry and Materials*, World Scientific, 2024, pp. 245–279.
- A. Y. Zueva, A. N. Bilyachenko, I. S. Arteev, V. N. Khrustalev, P. V. Dorovatovskii, L. S. Shul'pina, N. S. Ikonnikov, E. I. Gutsul, K. G. Rahimov, E. S. Shubina, N. Reis Conceição, K. T. Mahmudov, M. F. C. Guedes da Silva and A. J. L. Pombeiro, *Chem. – Eur. J.*, 2024, e202401164.
- P. Loganathan, R. S. Pillai, A. Jennifer, E. Varathan, M. Kesavan and S. Shanmugan, *New J. Chem.*, 2023, **47**, 8439.
- Q. Shen, K. Sheng, Z.-Y. Gao, A. Bilyachenko, X.-Q. Huang, M. Azam, C.-H. Tung and D. Sun, *Inorg. Chem.*, 2024, **63**, 13022.
- G. S. Astakhov, V. N. Khrustalev, M. S. Dronova, E. I. Gutsul, A. A. Korlyukov, D. Gelman, Y. V. Zubavichus, D. A. Novichkov, A. L. Trigub, E. S. Shubina and A. N. Bilyachenko, *Inorg. Chem. Front.*, 2022, **9**, 4525.
- (a) C. Detoni, N. M. F. Carvalho, D. A. G. Aranda, B. Louis and O. A. C. Antunes, *Appl. Catal., A*, 2009, **365**, 281; (b) C. Würtele, O. Sander, V. Lutz, T. Waitz, F. Tuczek and S. Schindler, *J. Am. Chem. Soc.*, 2009, **131**, 7544; (c) P. Roy and M. Manassero, *Dalton Trans.*, 2010, **39**, 1539; (d) M. Sutradhar, E. C. B. A. Alegria, T. R. Barman, H. M. Lapa, M. F. C. Guedes da Silva and A. J. L. Pombeiro, *Inorg. Chim. Acta*, 2021, **520**, 120314.
- (a) A. N. Kulakova, A. N. Bilyachenko, A. A. Korlyukov, L. S. Shul'pina, X. Bantreil, F. Lamaty, E. S. Shubina, M. M. Levitsky, N. S. Ikonnikova and G. B. Shul'pin, *Dalton Trans.*, 2018, **47**, 15666; (b) A. N. Kulakova, V. N. Khrustalev, Y. V. Zubavichus, L. S. Shul'pina, E. S. Shubina, M. M. Levitsky, N. S. Ikonnikov, A. N. Bilyachenko, Y. N. Kozlov and G. B. Shul'pin, *Catalysts*, 2019, **9**, 154; (c) G. S. Astakhov, M. M. Levitsky, A. A. Korlyukov, L. S. Shul'pina, E. S. Shubina, N. S. Ikonnikov, A. V. Vologzhanina, A. N. Bilyachenko, P. V. Dorovatovskii, Y. N. Kozlov and G. B. Shul'pin, *Catalysts*, 2019, **9**, 701.
- (a) E. C. B. A. Alegria, M. Sutradhar and T. R. Barman, *Catalytic oxidation of VOCs to added value compounds under mild conditions, Catalysis for a Sustainable Environment: Reactions, Processes and Applied Technologies*, ed. A. J. L. Pombeiro, M. Sutradhar and E. C. B. A. Alegria, John Wiley & Sons, 1st edn, 2024, ch. 9, vol. 1, pp. 161–179, ISBN: 978-1-119-87052-4; (b) T. Pan, H. Deng, Y. Lu, J. Ma, L. Wang, C. Zhang and H. He, *Environ. Sci. Technol.*, 2023, **57**, 1123; (c) X. Zhou, X. Zhou, C. Wang and H. Zhou, *Chemosphere*, 2023, **313**, 137489.



- 19 D. Murindababisha, A. Yusuf, Y. Sun, *et al.* Current progress on catalytic oxidation of toluene: a review, *Environ. Sci. Pollut. Res.*, 2021, **28**, 62030–62060.
- 20 A. Krishnamurthy, B. Adebayo, T. Gelles, A. Rownaghi and F. Rezaei, *Catal. Today*, 2020, **350**, 100–119.
- 21 M. Song, L. Yu, L. B. Song, *et al.*, *Environ. Sci. Pollut. Res.*, 2019, **26**, 22284–22294.
- 22 (a) R. Xie, D. Lei, Y. Zhan, B. Liu, C. H. A. Tsang, Y. Zeng, K. Li, D. Y. C. Leung and H. Huang, *Chem. Eng. J.*, 2020, **386**, 121025; (b) S. Okunaka, H. Tokudome and Y. Hitomi, *J. Catal.*, 2020, **391**, 480–484.
- 23 (a) R. Liu, H. Song, B. Li, X. Li and T. Zhu, *Chemosphere*, 2021, **263**, 127893; (b) S. Yang, H. Yang, J. Yang, H. Qi, J. Kong, Z. Bo, X. Li, J. Yan, K. Cen and X. Tu, *Chem. Eng. J.*, 2020, **402**, 126154.
- 24 Y. Zhang, Y. Liu, S. Xie, H. Huang, D. G. Guo and H. Dai, *Environ. Int.*, 2019, **128**, 335–342.
- 25 (a) X. Chen, S. Cai, E. Yu, H. Jia, X. Chen, X. Chen, S. Cai, E. Yu, J. Chen and H. Jia, *Appl. Surf. Sci.*, 2019, **475**, 312–324; (b) L. Zhao, Z. Zhang, Y. Li, X. Leng, T. Zhang, F. Yuan, X. Niu and Y. Zhu, *Appl. Catal., B*, 2019, **245**, 502–512.
- 26 (a) S. Dong, T. Chen, F. Xu, H. Liu, C. Wang, Y. Zhang, M. Ji, C. Xu, C. Zhu, Z. Li and X. Zou, *Catalysts*, 2022, **12**, 763; (b) M. Zang, C. Zhao, Y. Wang and S. Chen, *J. Saudi Chem. Soc.*, 2019, **23**(6), 645–654.
- 27 Y. Wang, H. Arandiyani, Y. Liu, Y. Liang, Y. Peng, S. Bartlett, H. Dai, S. Rostamnia and J. Li, *ChemCatChem*, 2018, **10**, 3429–3434.
- 28 L. F. Liotta, *Appl. Catal., B*, 2010, **100**, 403–412.
- 29 (a) R. Sanchis, D. Alonso-Domínguez, A. Dejoz, M. P. Pico, I. Álvarez-Serrano, T. García, M. L. López and B. Solsona, *Materials*, 2018, **11**, 1387; (b) J. Brunet, E. Genty, C. Barroo, F. Cazier, C. Poupin, S. Siffert, D. Thomas, G. De Weireld, T. Visart de Bocarmé and R. Cousin, *Catalysts*, 2018, **8**, 64.
- 30 (a) Y. Xu, Z. Qu, Y. Ren and C. Dong, *Appl. Surf. Sci.*, 2021, **560**, 149983; (b) G. Chen, K. You, F. Hao, *et al.*, *Res. Chem. Intermed.*, 2022, **48**, 2593–2606; (c) G. Chen, K. You, X. Gong, F. Zhao, Z. Chen and H. Luo, *React. Chem. Eng.*, 2022, **7**, 898–907.
- 31 (a) Y. Guo, M. Wen, G. Li and T. An, *Appl. Catal., B*, 2021, **281**, 119447; (b) X. Zhang, J. Zhao, Z. Song, H. Zhao and W. Liu, *Chem. Sel.*, 2019, **4**, 8902–8909; (c) B. Zhu, Y. Yan, M. Li, X.-S. Li, J.-L. Liu and Y. Zhu, *Plasma Processes Polym.*, 2018, **15**, 1700215; (d) L. Torrente-murciano, B. Solsona, S. Agouram and R. Sanchis, *Catal. Sci. Technol.*, 2017, **7**, 2886–2896.
- 32 (a) W. Liu, W. Xiang, N. Guan, R. Cui, H. Cheng, X. Chen, Z. Song, X. Zhang and Y. Zhang, *Sep. Purif. Technol.*, 2021, **278**, 119590; (b) T. Gan, X. Chu, H. Qi, W. Zhang, Y. Zou, W. Yan and G. Liu, *Appl. Catal., B*, 2019, **257**, 117943; C. Zhang, C. Wang, H. Huang, K. Zeng, Z. Wang, H.-P. Lia and X. Li, *Appl. Surf. Sci.*, 2019, **486**, 108–120; (c) B. Jiang, K. Xu, J. Li, H. Lu, X. Fei, X. Yao, S. Yao and Z. Wu, *J. Hazard. Mater.*, 2021, **405**, 124203.
- 33 (a) W. I. Abdel-Fattah, M. M. Eid, S. I. Abd El-Moez, E. Mohamed and G. W. Ali, *Life Sci.*, 2017, **183**, 28–36; (b) Y. Li, F. Liu, Y. Fan, G. Cheng, W. Song and J. Zhou, *Appl. Surf. Sci.*, 2018, **462**, 207–212; (c) S. Mo, Q. Zhang, Y. Sun, M. Zhang, J. Li, Q. Ren, M. Fu, J. Wu, L. Chen and D. Ye, *J. Mater. Chem. A*, 2019, **7**, 16197.
- 34 (a) N. Prigyi, S. Chanmungkalakul, V. Ervithayasuporn, N. Yodsin, S. Jungstittiwong, N. Takeda, M. Unno, J. Boonmak and S. Kiatkamjornwong, *Inorg. Chem.*, 2019, **58**, 15110; (b) M. Laird, C. Totée, P. Gaveau, G. Silly, A. van der Lee, C. Carcel, M. Unno, J. M. Bartlett and M. Wong Chi Man, *Dalton Trans.*, 2021, **50**, 81.
- 35 (a) G. S. Astakhov, A. N. Bilyachenko, M. M. Levitsky, L. S. Shul'pina, A. A. Korlyukov, Y. V. Zubavichus, V. N. Khrustalev, A. V. Vologzhanina, E. S. Shubina, P. V. Dorovatovskii and G. B. Shul'pin, *Inorg. Chem.*, 2020, **59**, 4536; (b) A. N. Bilyachenko, E. I. Gutsul, V. N. Khrustalev, G. S. Astakhov, A. Y. Zueva, Y. V. Zubavichus, M. V. Kirillova, L. S. Shul'pina, N. S. Ikonnikov, P. V. Dorovatovskii, E. S. Shubina, A. M. Kirillov and G. B. Shul'pin, *Inorg. Chem.*, 2022, **61**, 14800; (c) A. N. Bilyachenko, V. N. Khrustalev, A. Y. Zueva, E. M. Titova, G. S. Astakhov, Y. V. Zubavichus, P. V. Dorovatovskii, A. A. Korlyukov, L. S. Shul'pina, E. S. Shubina, Y. N. Kozlov, N. S. Ikonnikov, D. Gelman and G. B. Shul'pin, *Molecules*, 2022, **27**, 6205.
- 36 A. N. Bilyachenko, V. N. Khrustalev, G. S. Astakhov, A. Y. Zueva, I. S. Arteev, Y. V. Zubavichus, A. A. Korlyukov, P. V. Dorovatovskii, L. S. Shul'pina, N. S. Ikonnikov, M. V. Kirillova, E. S. Shubina, Y. N. Kozlov, A. M. Kirillov and G. B. Shul'pin, *Organometallics*, 2023, **42**, 2577.
- 37 M. N. Kopylovich, A. P. C. Ribeiro, E. C. B. A. Alegria, N. M. R. Martins, L. M. D. R. S. Martins and A. J. L. Pombeiro, *Adv. Organomet. Chem.*, 2015, **63**, 91, ch. 3.
- 38 M. S. S. Adam, A. Khalil, A. Taha, M. M. Mostafa, M. M. Makhlof and H. A. Mahmoud, *Surf. Interfaces*, 2023, **39**, 102914.
- 39 M. S. S. Adam, A. Khalil, A. Taha, M. M. Mostafa and M. M. Makhlof, *ACS Appl. Nano Mater.*, 2023, **6**(10), 8515–8528.
- 40 M. F. I. Al-Hussein and M. S. S. Adam, *Appl. Organomet. Chem.*, 2020, **34**, e5598.
- 41 A. K. Liubymova, T. V. Bezbozhnaya and V. L. Lobachev, *Kinet. Catal.*, 2021, **62**, 342.
- 42 (a) M. Sutradhar, E. C. B. A. Alegria, T. R. Barman, M. F. C. Guedes da Silva, C.-M. Liu and A. J. L. Pombeiro, *Front. Chem.*, 2020, **8**, 157; (b) M. Sutradhar, T. R. Barman, E. C. B. A. Alegria, M. F. C. Guedes da Silva, C.-M. Liu, H.-Z. Kou and A. J. L. Pombeiro, *Dalton Trans.*, 2019, **48**, 12839; (c) Z. Ma, Q. Wang, H. Yang, E. C. B. A. Alegria, M. F. C. Guedes da Silva, L. M. D. R. S. Martins, J. P. Telo, I. Correia and A. J. L. Pombeiro, *Catalysts*, 2019, **9**, 424; (d) M. Sutradhar, E. C. B. A. Alegria, M. F. C. Guedes da Silva, C.-M. Liu and A. J. L. Pombeiro, *Molecules*, 2018, **23**, 2699.

- 43 (a) W. N. R. W. Isahak and A. Al-Amiery, *Green Technol. Sustainability*, 2024, **2**, 100078; (b) J.-B. Feng and X.-F. Wu, *Appl. Organomet. Chem.*, 2015, **29**, 63.
- 44 (a) A. N. Bilyachenko, E. I. Gutsul, V. N. Khrustalev, P. V. Dorovatovskii, E. S. Shubina, Y. Guari, G. Félix, J. Larionova, A. G. Mahmoud and A. J. L. Pombeiro, *Cryst. Growth Des.*, 2023, **23**, 8707; (b) M. Sutradhar, E. C. B. A. Alegria, T. R. Barman, H. M. Lapa, M. F. C. Guedes da Silva and A. J. L. Pombeiro, *Inorg. Chim. Acta*, 2021, **520**, 1; (c) M. Sutradhar, M. G. Martins, D. H. B. G. O. R. Simões, R. M. N. Serôdio, H. M. Lapa, E. C. B. A. Alegria, M. F. C. G. da Silva and A. J. L. Pombeiro, *Appl. Catal., A*, 2022, **638**, 118623.
- 45 G. B. Shul'pin, *J. Mol. Catal. A: Chem.*, 2002, **189**, 39.
- 46 H. E. B. Lempers and R. A. Sheldon, *J. Catal.*, 1998, **175**(1), 62–69.
- 47 (a) K. Nomiya, K. Hashino, Y. Nemoto and M. Watanabe, *J. Mol. Catal. A: Chem.*, 2001, **176**, 79; (b) Z. Salta, A. M. Kosmas, M. E. Segovia, M. Kieninger, N. Tasinato, V. Barone and O. N. Ventura, *J. Phys. Chem. A*, 2020, **124**, 5917.
- 48 (a) G. B. Shul'pin and Y. N. Kozlov, *Org. Biomol. Chem.*, 2003, **1**, 2303; (b) G. B. Shul'pin, *C. R. Chim.*, 2003, **6**, 163.
- 49 M. Ghorbanloo, A. Mohamadi and H. Yahiro, *Nanochem. Res.*, 2016, **1**, 118.
- 50 M. Sutradhar, E. C. B. A. Alegria, T. Roy Barman, F. Scorcelletti, M. F. C. Guedes da Silva and A. J. L. Pombeiro, *Mol. Catal.*, 2017, **439**, 224.